Stochastic Sampling for Mantle Conductivity Models

Josef Pek[(1)], Jana Pěčová[(1)], Václav Červ[(1)] and Michel Menvielle[(2)]

[(1)]Institute of Geophysics, Acad. Sci. Czech Rep., v.v.i., Prague, Czech Republic
[(2)]CNRS CEETP, Saint Maur des Fossés, France

Abstract

We present a bayesian Monte Carlo analysis of geomagnetic induction data for the mantle conductivity distribution. We use a modified version of the Monte Carlo method with Markov chains based on an effective, data adaptive Metropolis sampling approach, and simulate samples from the posterior probability distribution of the resistivities in the mantle for four recently published global, regional, and satellite induction data sets. Stochastic sampling provides comprehensive maps of the parameter space based on fairly ranking the models according to their ability to explain the experimental data, as well as on respecting the prior information on the model parameters. From four generally formulated and tested priors for the mantle resistivities, the non-informative distribution on strictly increasing conductance is the most non-restricting prior that, at the same, avoids the non-likely high-resistivity tails from the marginal resistivity distributions. A prediction power of the MCMC sampling approach is demonstrated by a comparison of published maximum likelihood bounds on average conductivities in specific mantle zones with those produced simply by computing the average conductivities from the Markov chain of models.

1 Introduction

The electrical conductivity in the Earth's mantle is a particularly important parameter for studies of the temperature distribution, mineralogical composition and fluid content in the mantle. Carrying on the classical works by Banks (1969), Roberts (1984), Schultz and Larsen (1987), and others, new induction responses have been obtained in recent decades based either on largely extended data series and new methods and processing techniques (e.g., Olsen, 1998, 1999a; Honkura and Matsushima, 1998; Semenov, 1998; Schmucker, 1999; Semenov and Jóźwiak, 1999; Praus *et al.*, 2004), or on thoroughly re-assessed responses from earlier mantle conductivity studies (e.g., Constable, 1993; Medin *et al.*, 2007). New geomagnetic data from satellites have further extended the range of induction responses of the Earth both as regards the frequency spectrum and spatial coverage of the Earth (e.g., Olsen, 1999b; Constable and Constable, 2004; Kuvshinov and Olsen, 2006; Velímský *et al.*, 2006).

Based on the derived induction responses a number of mantle conductivity models have been suggested that revealed and refined the basic features of the electrical conductivity distribution in the Earth's mantle. Extremal D^+ models (Parker, 1980) have been studied to test the compatibility of the induction data with the 1-D hypothesis on the conductivity distribution, as well as to estimate the smallest misfit achievable within the 1-D model approximation (e.g., Constable, 1993; Olsen, 1999a). D^+ models are useful theoretical tools, but are non-physical by nature. Models with few uniform thick layers (e.g., Banks, 1969; Larsen, 1975; Olsen, 1998) are an option if it is reasonable to assume that a piecewise constant conductivity distribution with depth is an acceptable approximation to the true conductivity structure. In the Earth's mantle, however, the exponential conductivity vs. temperature dependence rather suggests to employ smoothly varying conductivity vs. depth models, even in those parts of the mantle that are assumed uniform as to their mineral composition.

Regularized Occam approach (Constable *et al.*, 1987) aims at restoring the simplest, minimum structure that is still compatible with the experimental data. The simplicity can be defined in various ways, which may accent some particular features of the restored models, the most common being the minimum norm that minimizes the distance from a pre-defined model, or the minimum gradient or minimum Laplacian norms that produce the smoothest models fitting the data (e.g., Constable, 1993; Olsen 1998, 1999a; Semenov, 1998; Semenov and Jóźwiak, 1999). Other structural penalties have been suggested as well aimed at, e.g., minimizing the total variation of the conductivity profile, the spatial extent of anomalous domains (minimum support norm), or the number of conductivity jumps within the model (minimum gradient support norm, Portniaguine and Zhdanov, 1999).

Stochastic inversion methods provide alternatives to conventional non-linear inverse procedures. They scan the model parameter space and identify multiple models that match a given dataset, thus providing additional

information on parameter uncertainty. Grandis *et al.* (1999) suggested using a bayesian Markov chain Monte Carlo (MCMC) approach to the solution of a 1-D magnetotelluric inverse problem, with the model parametrization similar to that used in traditional linearized Occam inversions. Bayesian approach not only produces maps of data matching models in the parameter space, it also ranks the models and calculates posterior model probabilities conditioned on the observed data. While neither analytical, nor direct search, nor random shooting approaches are feasible strategies to restoring the probability distributions in a multi-parametric magnetotelluric inverse problem, the MCMC is a technique that allows simulating a sample from the posterior probability distribution numerically in a computationally feasible way.

The aim of this paper is to demonstrate and discuss results of application of the bayesian MCMC to the inversion of global geomagnetic induction data for mantle electrical conductivity. We will especially address two aspects of this problem, specifically (i) the impact of the data quality on the probabilistic inversion, and, (ii) the role prior information on the model parameters plays in the inversion results. The structure of the paper is as follows: In Section 2, we give a brief outline of the bayesian MCMC approach as we apply it in this study. Section 3 characterizes four global and regional induction data sets, previously published, which we have used in the MCMC experiments. In Section 4, we present the MCMC sampling results for the mantle conductivity obtained for the four data sets under various common prior assumptions as to the model parameters in the Earth. Section 5 concludes the study by comparing our MCMC results with conductivity models presently available.

2 Bayesian Stochastic Sampling

In a bayesian approach, both the parameter estimation and the assessment of the parameter uncertainties are treated as problems of determining the posterior probability of parameters of the conductivity model conditioned on the observed induction response data. If a model class is specified, say M, then our knowledge on the model parameters, $\mathbf{m}$, prior to the experiment, formalized as a prior probability $\mathrm{Prob}(\mathbf{m}|M)$, can be updated by employing the experimental data, $\mathbf{d}^{\mathrm{exp}}$, according to the Bayes rule,

$$\mathrm{Prob}(\mathbf{m}|\mathbf{d}^{\mathrm{exp}}, M) = \frac{\mathrm{Prob}(\mathbf{d}^{\mathrm{exp}}|\mathbf{m}, M)\,\mathrm{Prob}(\mathbf{m}|M)}{\mathrm{Prob}(\mathbf{d}^{\mathrm{exp}}, M)}, \tag{1}$$

(see, e.g., Gelman *et al.*, 2004). Here, the probability function $\mathrm{Prob}(\mathbf{d}^{\mathrm{exp}}|\mathbf{m}, M)$ is the likelihood, and specifies how likely a model with parameters $\mathbf{m}$ is to produce the particular set of observed data $\mathbf{d}^{\mathrm{exp}}$. The posterior probability density function $\mathrm{Prob}(\mathbf{m}|\mathbf{d}^{\mathrm{exp}}, M)$ is considered a solution to the inverse problem, and can be further used in assessing the parameters, evaluating point estimates, confidence intervals, etc.

Provided the noise in the experimental data is normal Gaussian with standard deviations $\delta\mathbf{d}^{\mathrm{exp}}$ and the data items are mutually independent, the likelihood in (1) can be written

$$\mathrm{Prob}(\mathbf{d}^{\mathrm{exp}}|\mathbf{m}, M) \propto \exp\left[-\sum_{j=1}^{N_D} \left(\frac{d_j^{\mathrm{exp}} - d_j^{\mathrm{mod}}(\mathbf{m})}{\delta d_j^{\mathrm{exp}}} \right)^2 \right], \tag{2}$$

where N_D is the number of individual data items, and $\mathbf{d}^{\mathrm{mod}}(\mathbf{m})$ is a solution to the direct problem for the parameters $\mathbf{m}$. The nominator $\mathrm{Prob}(\mathbf{d}^{\mathrm{exp}}, M)$ in (1) is a normalization constant independent of $\mathbf{m}$ and need not be considered explicitly in cases where only model ranking is requiered.

In this study, the model class M is defined by a spherically symmetric model with a conductive mantle reaching from the surface down to the depth of 2900 km, and with a perfectly conducting core between the bottom of the mantle and the centre of the Earth at $R_E = 6371$ km. The crust and mantle portion of the model consists of a uniform crust, thickness $h_c = 30$ km, and a suite of thin layers with fixed, log-uniform thicknesses throughout the mantle. The variables for the inversion are the logarithm of the resistivity of the crust, $\varrho_c \equiv \varrho_1$, and logarithms of the resistivities of the individual mantle layers, $\varrho_2, \ldots, \varrho_L$, where L is the total number of layers. Typically, we have used $L = 61$ in most of our experiments. To solve the direct problem for the finely stratified mantle, we employed the standard 1-D direct magnetotelluric algorithm for stratified conductors and further made use of the Weidelt's flattening transformation in our computations to account for the sphericity of the Earth (Weidelt, 1972; see also Olsen, 1999a).

The prior probability in (1), $\mathrm{Prob}(\mathbf{m}|M)$, describes the available knowledge about the layer resistivities prior to the data being observed, and this may be one of the most sensitive issues of a bayesian analysis, especially if no or only very limited information is available apriori.

A bayesian analysis requires the priors on the parameters to be specified explicitly in (1). As we wanted to understand the role the priors play in modulating the mantle conductivity models we have tested four sufficiently general priors for the layer resistivities in the mantle:

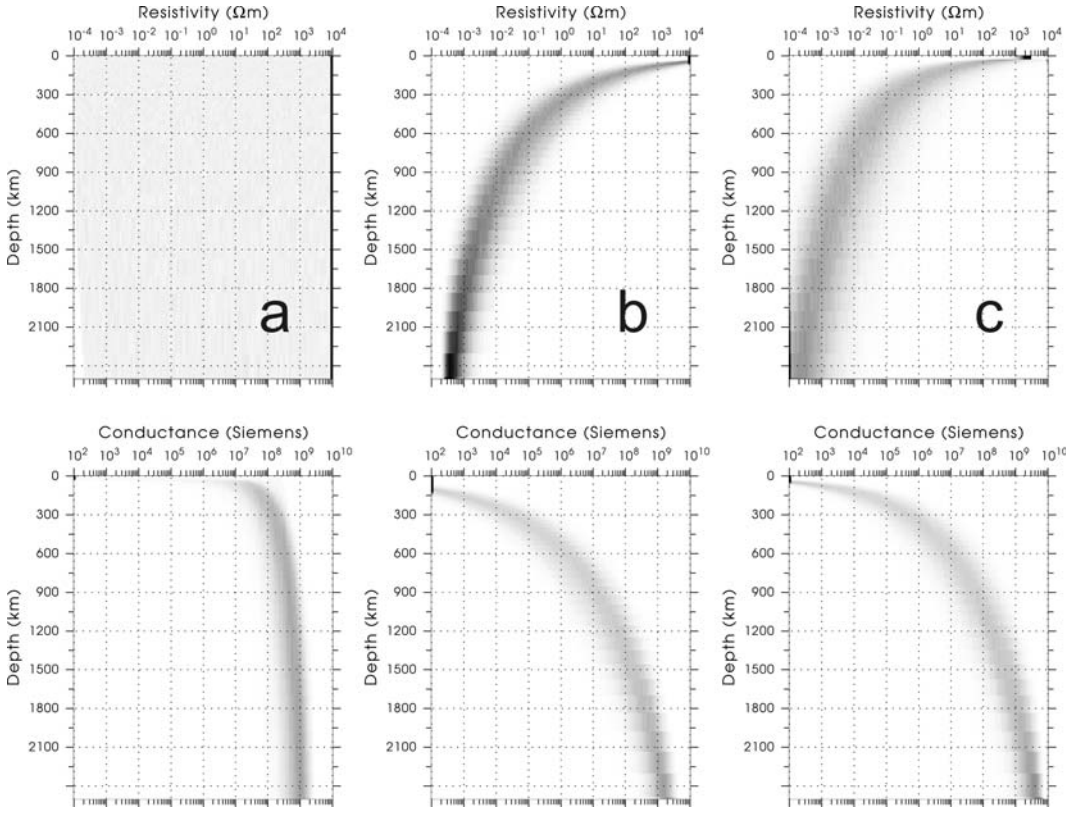

Figure 1: Gray shade maps of prior marginal probability density functions for the resistivities of the mantle layers in the $\log \varrho - z$ frames (top panes) and for conductances at the bottom of the mantle layers in the $\log S - z$ frames (bottom panes). The gray shade maps represent converted relative histograms approximating the marginal priors for the resistivities/conductances for each individual mantle layer. For the gray shade scale, white is for no occurrence and black for the occurrence in 10% or more cases for resistivities, and in 30% or more cases for conductances. a—Non-informative Jeffrey's prior on each layer resistivity, resistivities considered mutually independent (Pi in text), b—Prior for the case of the resistivities distributed uniformly within individual mantle layers, but non-increasing resistivity is required throughout the mantle (Piii in text), c—Prior for the case of the conductances at the bottom of individual mantle layers distributed uniformly, strictly increasing conductance is required throughout the mantle (Piv in text).

Pi) Without having carried out any induction experiments, we could not anticipate any specific mantle resistivity features, except perhaps for some loose resistivity bounds dictated by general physics. The prior that expresses total ignorance about a positive parameter, $\varrho_i > 0$, $\varrho^{\min} < \varrho_i < \varrho^{\max}$, is the Jeffrey's prior, $\ln \varrho_i \sim U(\ln \varrho^{\min}, \ln \varrho^{\max})$, $i = 1, \ldots, L$, where $U(a, b)$ is for a uniform distribution on the interval (a, b) (e.g., Ulrych *et al.*, 2001). If no relations between the layer resistivities are assumed apriori, the prior pdf on $\mathbf{m} = (\varrho_1, \ldots, \varrho_L)$ is constant and given by $\mathrm{Prob}(\mathbf{m}|M) = \ln^{-L} \varrho^{\max}/\varrho^{\min}$. The top panel in Fig. 1a shows, as histograms converted into gray scale maps, marginal priors for the individual resistivities ϱ_i, $i = 1, \ldots, L$, in the $\log \varrho$ vs. depth frame. The particular choice of the resistivity bounds was $\varrho^{\min} = 10^{-4}$ Ωm, $\varrho^{\max} = 10^5$ Ωm here. It is interesting that the prior for conductance, $S_i = \sum_{j=1}^{i} h_j/\varrho_j$, seems to prefer models with rapidly increasing conductance in the shallow part of the mantle in this case (Fig. 1a, bottom pane).

Pii) Even without any induction measurements, other geophysical parameters in the mantle suggest that the assumed independence between the layer resistivities is a weak point of the previous prior Pi. Specifying a correlation function between prior uncertainties can be used to enforce proper smoothing into the conductivity model, but that information is not available in practice. We use a simple prior by Haario *et al.* (2004) that is based on the assumption that the neighbouring discretized values of a resistivity profile cannot be too different, which can be formalized as, e.g., $\ln \varrho_{i+1} - \ln \varrho_i \sim N(0, \nu^2)$, where $N(\mu, \sigma^2)$ is for a normal pdf

with the mean μ and variance σ. Alternatively, second or higher order differences of $\ln \varrho$ can be used as well. By using in (1) this prior along with the likelihood (2), we have

$$\mathrm{Prob}(\mathbf{m}|\mathbf{d}^{\mathrm{exp}}, M) \propto \exp\left[-\sum_{j=1}^{N_D} \left(\frac{d_j^{\mathrm{exp}} - d_j^{\mathrm{mod}}(\mathbf{m})}{\delta d_j^{\mathrm{exp}}} \right)^2 - \frac{1}{2\nu^2} \sum_{k=1}^{L-1} (\ln \varrho_{k+1} - ln\varrho_k)^2 \right], \qquad (3)$$

which formally gives the Occam first derivative smoothed solution, with the structure penalty weight $\lambda = 1/2\nu^2$, as a maximum aposteriori probability (MAP) estimate. This smoothing prior does not allow a simple visualization and is therefore omitted in Fig. 1.

Piii) The third prior is identical with the non-informative Pi above except that strictly non-decreasing resistivity is required throughout the mantle, $\varrho_{i+1} \leq \varrho_i,\ i = 1, \ldots, L-1$, an assumption used as an option by Medin *et al.* (2007) in their study on average conductivities in selected mantle domains. This prior (Fig. 1b) shows rather a strong regularizing effect. The marginals in Fig. 1b can be made more uniform and their maxima less pronounced if the resistivity bounds ($\varrho^{\min}$, $\varrho^{\max}$) are broadened. This, however, has technical disadvantages since it increases the volume of the parameter space, and necessarily also the computation demads of the MCMC sampling.

Piv) The fourth prior is similar to the previous one, but is formulated for the conductances at the bottom of the mantle layers, $S_i = \sum_{j=1}^{i} h_j/\varrho_j,\ i = 1, \ldots, L$. Here, we assume that $\ln S_i \sim U(\ln S^{\min}, \ln S^{\max})$ and $S_{i+1} > S_i$ for any i (see Fig. 1c for the conductance bounds $10 < S_i < 10^{10}$, in siemens).

Grandis *et al.* (1999) used the MCMC method with a standard Gibbs sampler to simulate samples from the posterior pdf (1). In this approach, the domain under study is scanned successively in a component-by-component way, and an ergodic Markov chain is designed with the invariant distribution equal to the posterior pdf (1). After a large enough sample from the posterior probability density function has been obtained, basic bayesian integrals for the means, covariance matrices, etc., can be easily evaluated from the posterior sample and used to assess the resistivity models as well as their uncertainties.

We have used a slightly less demanding sampling procedure based on the single component adaptive Metropolis procedure (SCAM, Haario *et al.*, 2003) which proceeds in similar cycles as the Gibbs sampler except that the updates to the individual components are generated by a data adaptive Metropolis rule. As in this algorithm a longer history of the chain is used for adapting the variances for the Metropolis step, the chain is evidently not Markovian any more. Nonetheless, Haario *et al.* (2003) have proved its convergence to the target posterior under sufficiently general conditions. More details on a general theory as well as on particular aspects of our MCMC implementation can be found, e.g., in (Gelman *et al.*, 2004; Grandis *et al.*, 1999; Haario *et al.*, 2003; Červ*et al.*, 2005).

3 Data Sets for Mantle Conductivity Studies

To compare the effect of the stochastic sampling approach in the inversion of induction responses of different origin and different quality, we have applied the bayesian MCMC sampling technique to four different sets of induction responses published in recent years. In particular, we have dealt with the following data sets:

Summarized Representative Responses by Medin et al. (2007)

Medin *et al.* (2007) used a 34 admittance set of data that is a combination of Constable's (1993) global responses averaged and statistically re-assessed from previous data by Roberts (1984) and Schultz and Larsen (1987), and of data by Olsen (1999a) from land observatories in Europe. Prior to the modeling, the data were checked for a 1-D compatibility by assessing misfit of the extremal D^+ solution. Data that contributed most to the violation of the 1-D hypothesis have been removed from the set. The thorough analysis and selection of individual data items into this data set justify our taking this admittance collection as a reference data set.

Standard Global Responses for Sq and Long Period Variations by Praus et al. (2004)

Praus *et al.* (2004) presented a standard set of 13 global induction response data for two period ranges. Specifically, they studied the Sq daily variation data from 88 to 94 land observatories over the globe for the IQSY year 1965. Additionally, they processed data for long period variations, within the period range of 4 days up to 1 year, from 40 to 48 world observatories independently in three 3-years segments with largely different solar and geomagnetic activities (1958-60, 1963-65, 1967-69) by the standard Z/H-method. The data were supplemented by the 11-year response estimate by Harwood and Malin (1977). The global non-robust processing approach used in the study by

Praus *et al.* (2004) necessarily produced data with larger variance as compared to other data sets used. Moreover, the data collection is discontinuous as it does not involve data from the range of Dst transients.

Magnetic Variation Response for North-Central Europe by Semenov (1998)

Semenov (1998) published local impedances from magnetic variation studies over several regions all over the world. We consider here his averaged induction response for the region of North-Central Europe, roughly involving the geologically intricate territory of a broader vicinity of the Trans-European Suture Zone. The data set consists of 16 complex impedances within the period range of about 4 hours to 3.7 years. At the high frequency end, the data are supplemented by 3 impedance values from long period magnetotelluric studies, extending thus the period range down to 20 minutes. At the lowest frequencies, this data set has also been supplemented by the 11-year response estimate by Harwood and Malin (1977).

Satellite Geomagnetic Induction Responses by Kuvshinov and Olsen (2006)

Kuvshinov and Olsen (2006) processed five years (2001-2005) of scalar and vector magnetic field measurements from the Ørsted and CHAMP satellites, and scalar magnetic field measurements from the SAC-C satellite. They published a set of 17 complex values of the C-response function within the period range of about 14 hours to 143 days. As the inhomogeneous, highly conducting ocean may affect the induction data considerably, the authors developed and applied a scheme for correcting for the effect of induction in the non-uniform oceans. The main distorting effect of the ocean occurs at periods up to 7 days, and after the correction has been made, the satellite responses suggest upper mantle conductivities similar to those obtained from ground-based data. Here, we have used only the corrected response set by Kuvshinov and Olsen (2006).

4 Mantle Conductivity Models via Stochastic Sampling

For each of the data sets listed in the previous section, we have carried out several MCMC sampling runs with the priors suggested in Section 2. A typical setting of an MCMC (SCAM) run was: 1 million iteration steps; from those the first 100000 steps were considered a burn-in phase and discarded from the analysis. According to a typical behavior of the parameter autocorrelations along the chain, we only considered each 100-500th model from the chain to reduce the dependence between the sample elements. It is in general difficult to assess convergence of the MCMC sampling, though theoretically it is guaranteed. We have relied on two diagnostic criteria in this respect, the stabilization of the chain over a large number of iteration steps and, in a few experiments with several parallel chains running, similarity of the inter-chain and within-the-chain parameter variances.

In an analogous way as for the prior pdf's in Fig. 1, we also present the histograms, converted into gray scale maps, approximating the posterior marginal pdf's for the resistivities of the individual mantle layers as well as the conductances at their bottoms. The histograms are constructed from the sample parameters generated by the SCAM algorithm applied to the posterior (1) with the Jeffrey's prior on entirely non-correlated layer resistivities considered. As expected, the histograms show considerable occurrence of the resistivity values in the high-resistivity sections of the maps, indicating that many of the models in the sample may oscillate wildly, with practically no limit on the resistivity from above. From below, the resistivities are limited by about 10 Ωm between 100 to about 400 km in models Fig. 2a, b and d (global observatory data by Medin *et al.*, 2007, and by Praus *et al.*, 2004, and satellite data by Kuvshinov and Olsen, 2006, respectively), while the regional data by Semenov (1998) shift the lower resistivity envelope towards 2-3 Ωm between 200 and 400 km, and suggest a more conductive structure to exist at those depths (Fig. 2c). Below 400 km the minimum resistivity envelope decreases rapidly in all models, to about 1 Ωm at 600 km and to values around 0.1 Ωm at 800 km. Within the depth range of 400 to 900 km, several marked spots of increased probability are observed, especially well developed in the maps based on the high-quality data by Medin *et al.* (2007) and on the satellite data by Kuvshinov and Olsen (2006) in Figs. 2a and d, respectively. Those spots seem to partly correspond to the δ-peaks of the respective D^+ solutions overlaid on the probability maps in Fig. 2. It seems to be a logical relation, as an inversion for unconstrained 1-D resistivity should tend to produce a D^+-like solution. Below 900 km, an almost constant minimum resistivity profile is indicated by Fig. 2a, with one more spot of increased probability between about 1150 and 1350 km, which cannot be distinguished in any other of the models presented. The slow decrease of the minimum resistivity in the lower mantle in Figs. 2b, c may already indicate insufficient resolution of the data, and increased attraction of the models to the prior distribution deep in the mantle, which then seems to take almost a full control over the resistivities below the depth of about 2000 km, and even earlier, at about 1500 km, for the satellite data.

The assess the adequacy of the posterior probability samples generated by the SCAM process to the experimental data, we may compare the pdf's of the model responses from the chain with the stochastic model of the experimental data. Though the responses of the models from the SCAM chain should replicate the pdf's of the experimental data after a sufficiently long run, and exact tests for the goodness-of-fit could be arranged, we will

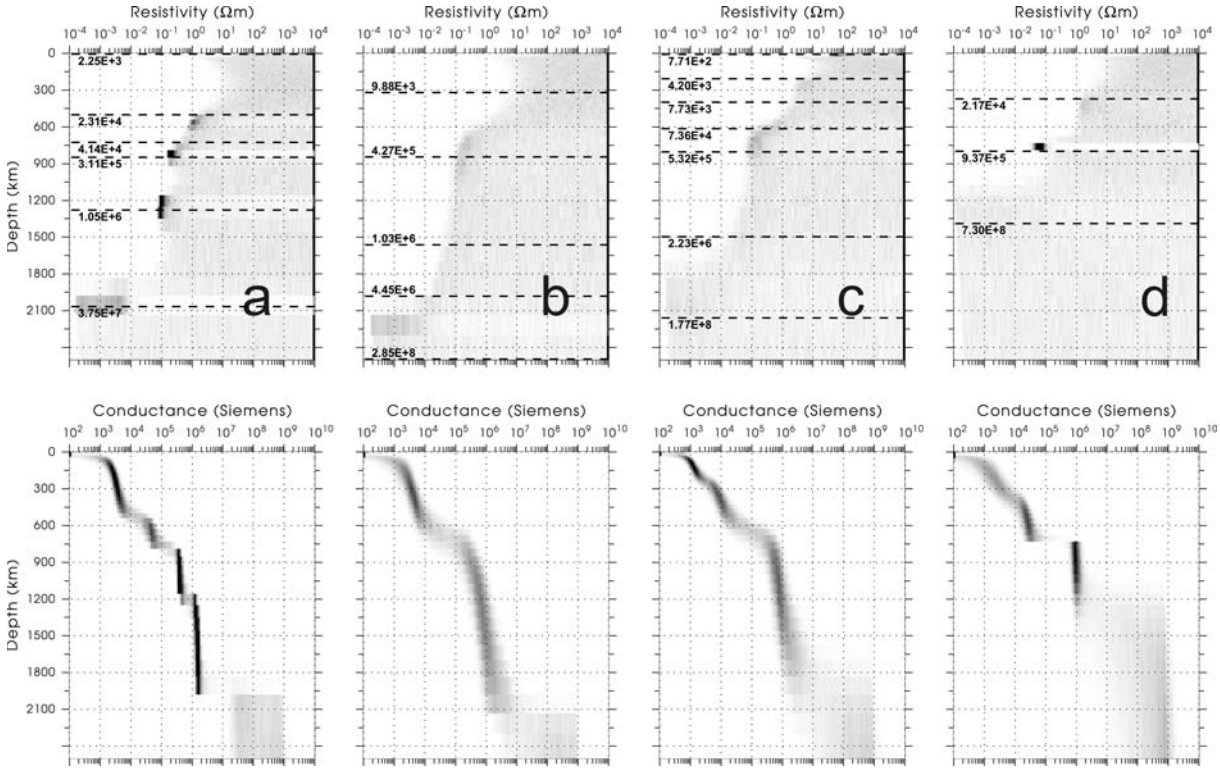

Figure 2: Gray shade maps of marginal probabilities of the resistivities of the mantle layers from a SCAM sample generated from the non-informative prior Pi (Section 2) and the four data sets listed in Section 3, specifically, for data by a—Medin *et al.* (2007), b—Praus *et al.* (2004), c—Semenov (1998), d—Kuvshinov and Olsen (2006). The gray shade maps represent converted relative histograms approximating the marginal posteriors for the resistivities/conductances for each individual mantle layer. For the gray shade scale, white is for no occurrence, and black for the occurrence in 10% or more cases for resistivities (top panes), and in 30% or more cases for conductances (bottom panes). The dashed lines in the resistivity maps show the positions of the δ-peaks of the D^+ solution, and are labeled with the corresponding sheet conductances in siemens. RMS bounds for 90 per cent of all models in the SCAM chain, for model a: 1.254–1.335 (1.211), b: 0.550–0.853 (0.508), c: 0.609–0.859 (0.433), d: 1.354–1.508 (1.290). In the brackets, the RMS for the D^+ solution is given.

assess the model-to-data fit only qualitatively here. For this to do, we have added to the figure caption of Fig. 2, and later also to Figs. 3, 4, and 5, intervals of the RMS parameters (normalized by the data variances) for 90 per cent of all the models generated during the stabilized phase (after burn-in) of the chain.

Fig. 3 shows the posterior marginals for the resistivities in models generated by the SCAM algorithm under the smoothing prior Pii (see Section 2). In this case, we have to specify, in terms of the parameter ν in (3), how tense the link should be between neighboring layer resistivities. Though more sophisticated approaches might be suggested, we have taken the simplest way here by choosing ν apriori from the standard L-curve approach within a linearized Occam inversion run applied to the best data set by Medin *et al.* (2007). We have kept this particular value of ν also for the other data sets analyzed in order to guarantee that the same structural constraint is applied in all cases.

With the smoothing prior employed, the resistivity marginals simplify considerably, showing a steady resistivity decrease from about 100-500 Ωm at 150 km to 0.7-2 Ωm at 800 km, followed by a very slow resistivity decrease to about 0.3-0.6 Ωm at 1500 km. Beneath about 1300-1500 km, Fig. 3a, and to a less obvious degree also Fig. 3c, indicate a faster resistivity decrease in the lower mantle. This feature is not resolved by the other two data sets.

An almost one order of magnitude increase of the resistivity is suggested within the shallowest, 100-150 km thick section by models with the (first derivative) smoothing prior in Figs. 3a and c. Moreover, in the regional model from the Semenov's (1998) data in Fig. 3c, the separate conducting layer between about 200 and 300 km persists, which has been already indicated by sampling for the 'non-regularized' resistivities. Poorer short period data for Fig. 3b do not resolve any shallow features. Neither is the resistivity increase in the lithosphere indicated by the satellite data in Fig. 3d, but here the correction introduced by Kuvshinov and Olsen (2006) to eliminate the effect of the oceans might have affected that part of the induction response which is sensitive to shallow depths.

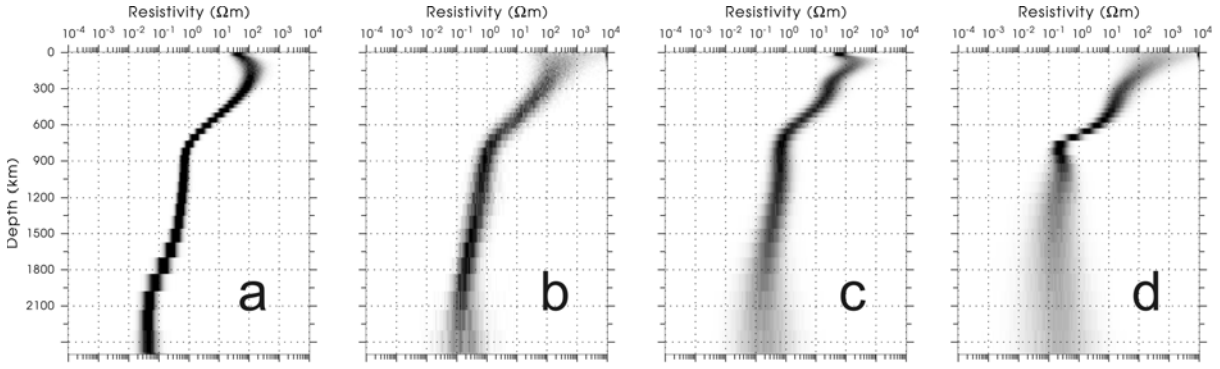

Figure 3: Gray shade maps of marginal probabilities of the resistivities of the mantle layers from a SCAM sample generated from the smoothing prior Pii (Section 2) and the four data sets listed in Section 3. RMS bounds for 90 per cent of all models in the SCAM chain, for model a: 1.369–1.475, b: 0.616–0.888, c: 0.645–0.872, d: 1.464–1.599. For the plot attributes, see caption to Fig. 2.

.

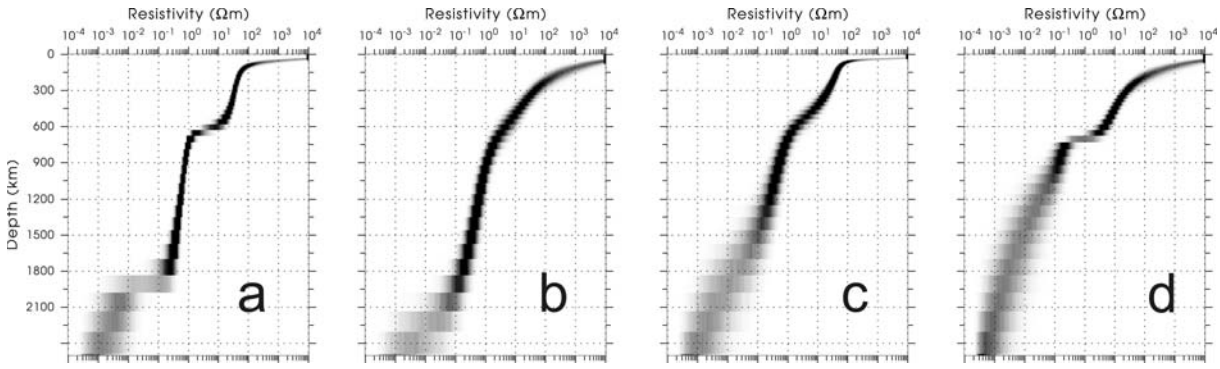

Figure 4: Gray shade maps of marginal probabilities of the resistivities of the mantle layers from a SCAM sample generated from the prior Piii requiring non-increasing resistivity throughout the mantle (Section 2) and the four data sets listed in Section 3. RMS bounds for 90 per cent of all models in the SCAM chain, for model a: 1.448–1.575, b: 0.653–0.913, c: 1.117–1.390, d: 1.481–1.607. For the plot attributes, see caption to Fig. 2.

The satellite model also suggests anomalously low resistivities, of the order of 0.1 Ωm, at mid-mantle depths, which contradicts the Occam model presented by Kuvshinov and Olsen (2006). This may be related to the particular choice of the smoothing parameter ν here. For the models in Fig. 3d, the RMS is between 1.464 and 1.599 for 90 per cent of the SCAM generated models, while Kuvshinov and Olsen (2006) report a misfit value which would correspond to the RMS of 1.78. In our MCMC experiments, ν would have to be decreased by a factor of 3 to 5 to achieve the same RMS range, which would flatten the model considerably in its mid-mantle section.

Requiring the resistivity to be a non-increasing function of depth throughout the mantle (prior Piii in Section 2) seems to be a strong regularizing factor, as can be seen from marginal resistivity histograms in Fig. 4. The models show only the main feature of a sharp resistivity decrease at mid-mantle depths of 600-700 km. We had difficulties with fitting properly the regional data set by Semenov (1998) under this prior, as systematic discrepancies between the model and experimental data occurred regularly at the shortest periods up to 2×10^4 s. It may indicate that a distinct conducting layer in the upper mantle is required by this particular data set, but some inconsistencies originating from merging the long period tensor magnetotelluric data with the scalar geomagnetic induction response in this period range cannot be excluded either. The shallow high resistivities for all models are required by the data under the Piii prior, and restricting the resistivity by a decreased $\varrho^{\max}$ increases the misfit (e.g., from 1.278–1.964 RMS for 90% of models at $\varrho^{\max} = 10^5$ Ωm to 1.905–2.189 at $\varrho^{\max} = 300$ Ωm for the data set by Medin *et al.*, 2007).

The prior Piv (Section 2), requiring a strictly increasing conductance throughout the mantle, may seem somewhat unproductive, since any conductance has to be an increasing function of depth, whatever the underlying resistivity distribution. But combined with the Jeffrey's uniformity condition on each $\ln S_i,\ i = 1, \ldots, L$, this prior seems to better conform our apriori belief on the mantle resistivity distribution in that it eliminates both the low and high-resistivity extreme domains from the resistivity pdf's without restricting the structure too much.

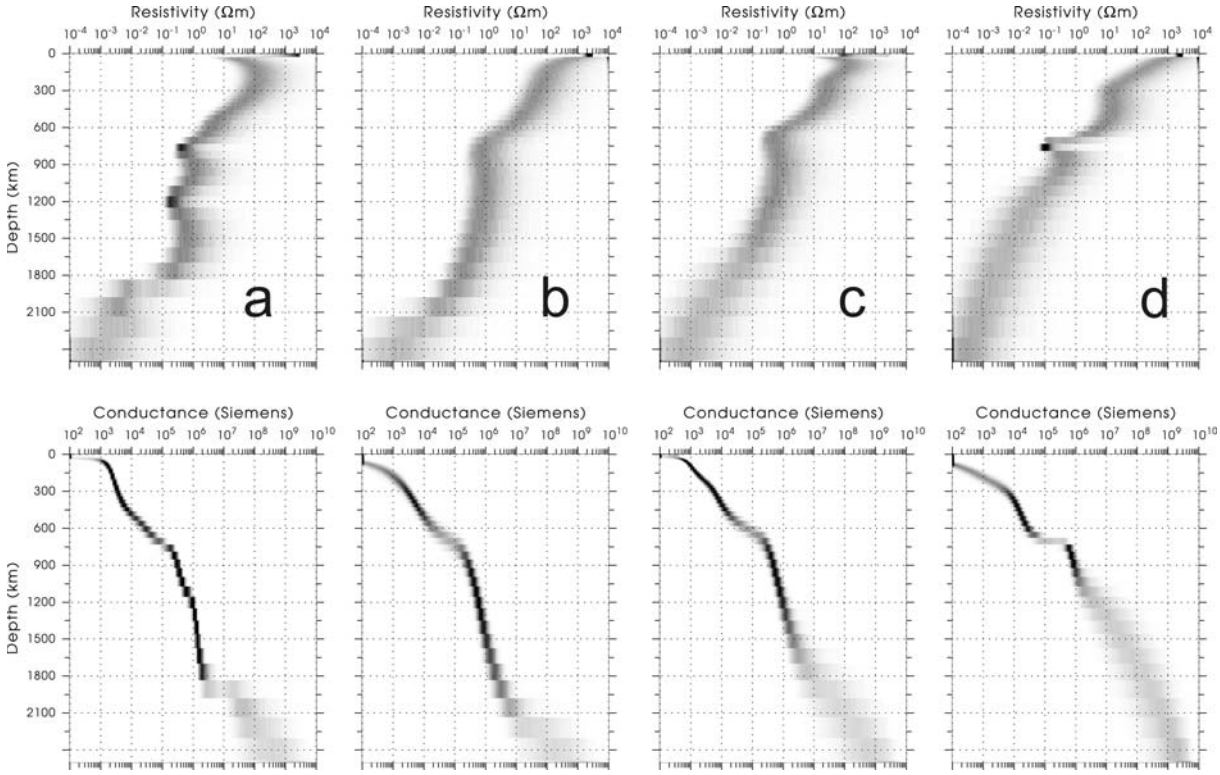

Figure 5: Gray shade maps of marginal probabilities of the resistivities of the mantle layers from a SCAM sample generated from the conductance prior Piv (Section 2) and the four data sets listed in Section 3. RMS bounds for 90 per cent of all models in the SCAM chain, for model a: 1.278–1.964, b: 0.518–0.734, c: 0.590–0.769, d: 1.380–1.513. For the plot attributes, see caption to Fig. 2.

Marginals of the resistivities and conductances from models sampled with this prior employed are shown in Fig. 5. They principally reproduce the conductivity features observed in Fig. 2 for independent layer resistivities, but are more effectively channelized, and do not show the long, most likely spurious, high-resistivity tails.

5 Conclusion

The numerical MCMC experiments with a 1-D inversion of geomagnetic induction responses for the mantle electrical conductivity have shown that the stochastic sampling can be considered a suitable tool for this kind of geophysical inverse problems. A relative simplicity of the underlying direct problem allows us to generate sufficiently representative samples from the posterior pdf and obtain representative marginal posterior pdf's for the resistivities in the mantle. As compared to standard linearized inverse approaches, stochastic sampling provides a more comprehensive map of the parameter space based on fairly ranking the models according to their likelihoods (i.e., according to the model-to-data fit), and with regard to the prior information available.

We have demonstrated the role of the prior pdf's by testing four sufficiently general prior types that may reflect our limited knowledge of the deep electrical structure of the Earth. We have applied the MCMC sampling to four different data sets, ranging from global ground-based data of different quality (Medin *et al.*, 2007; Praus *et al.*, 2004), through regional induction responses by Semenov (1998), through the latest satellite data by Kuvshinov and Olsen (2006). The averaged and thoroughly pre-assessed data set by Medin *et al.* (2007) has proved superior as to the resolution of the mantle conductivity structure. As regards the prior distributions, they show rather a strong effect on the final model parameter distributions. In particular, the smoothing and non-increasing resistivity priors, Pii and Piii in Section 2, show a strong regularizing effect, while the strictly-increasing-conductance prior, Piv in Section 2, may be employed if no extra smoothing/correlation is welcome and the high-resistivity tails of the resistivity marginals, most likely spurious, are to be avoided.

Bayesian analysis, and the MCMC as an efficient tool to carry it out practically, is an effective approach to predicting specific or derived features of models, as well as in cases when heterogeneous information is to be interpreted jointly. For the latter case, the study by Khan *et al.* (2006) on constraining the composition and thermal state of the mantle beneath Europe from inversion of long period electromagnetic sounding data is an excellent

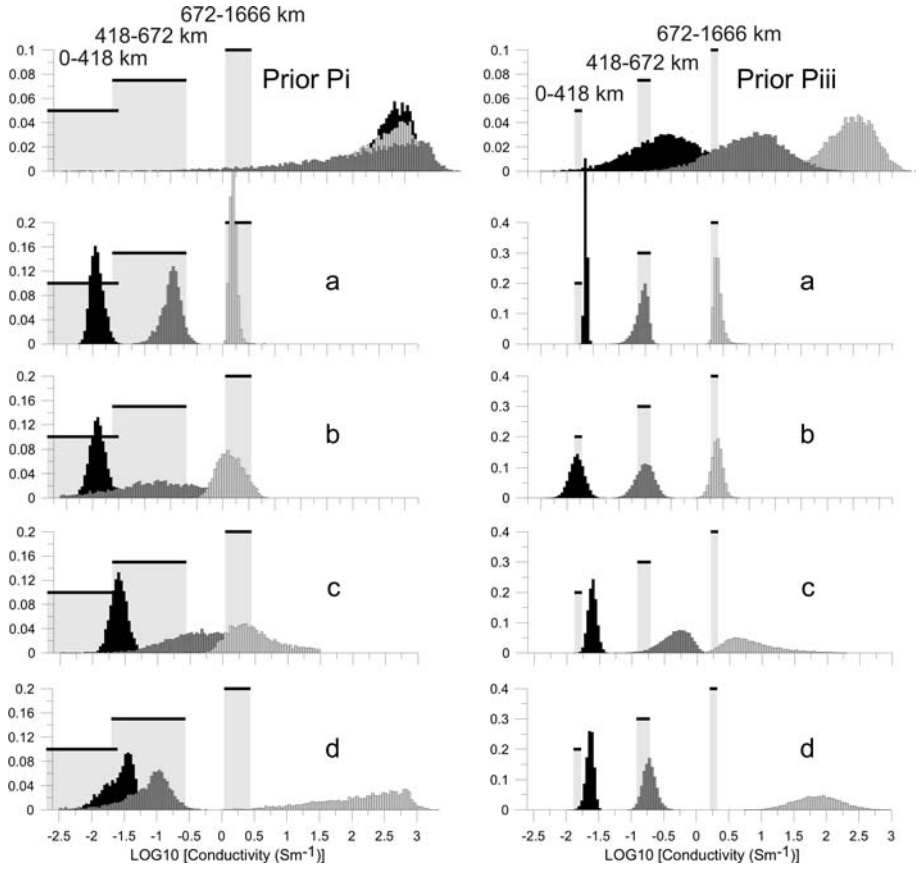

Figure 6: Comparison of ML estimates of average conductivities in three mantle domains, 0–418 km, 418–672 km, and 672–1666 km from Medin *et al.* (2007) with those predicted from the SCAM samples. Left column compares ML ranges of 90% χ^2 bounds on the average conductivity (light gray boxes) with histograms of the SCAM generated values under the non-informative prior Pi. Right column compares ML results obtained under the condition $d\sigma(z)/dz \geq 0$ with histograms from SCAM simulations under the non-increasing-resistivity prior Piii. The model labels, a–d, correspond to those in Fig. 2.

example. We present here, in Fig. 6, only a simple comparison of MCMC estimates of average conductivities in specific domains of the mantle with those obtained by a direct maximum likelihood (ML) inversion by Medin *et al.* (2007). The direct ML and MCMC ranges compare well for most of the models at the upper bound of the average conductivities, provided the mantle domain considered is sensed by the data. The difference in the predicted lower bounds for the case of the non-informative prior is mainly due to the fixed $\varrho^{\max} = 10^5$ Ωm, which rules out all acceptable models with extremely high-resistivity layers beyond that limit from the MCMC sample. Nonetheless, this example demonstrates that successful predictions are possible from the MCMC simulations, without much additional costs over and above those that are necessary for the basic MCMC runs.

Acknowledgment

The support of the Czech Sci. Found., under contract No. 205/06/0557, and the Grant Agency Acad. Sci. Czech Rep., under contract No. IAA200120701, to this study is highly acknowledged.

References

Banks, R., 1969, Geomagnetic variations and the electrical conductivity of the upper mantle, *Geophys. J. R. Astron. Soc.*, **17**, 457–487.

Constable, S. C., Parker, R. L. and Constable, C. G., 1987, Occam's inversion—A practical algorithm for generating smooth models from electromagnetic sounding data, *Geophysics*, **52** (03), 289–300.

Constable, S., 1993, Constraints on Mantle Electrical Conductivity from Field and Laboratory Measurements, *J. Geomag. Geoelectr.*, **45**, 707–728.

Constable, S. and Constable, C., 2004, Observing geomagnetic induction in magnetic satellite measurements and associated implications for mantle conductivity, *Geochem. Geophys. Geosyst.*, **5**, Q01006.

Červ, V., Pek, J. and Menvielle, M., 2005, Bayesian Monte Carlo for MT Tensor Decomposition, in *Proc. 21st Coll. Electromagnetic Depth Research*, Holle, Germany, Oct 3-7, 2005, Ritter, O. and Brasse, H. (Eds.), pp. 146–155.

Haario, H., Saksman, E. and Tamminen, J., 2003, Componentwise adaptation for MCMC, *Rep. Dept. Math.*, Univ. Helsinki, prepr. 342, pp. 1–20.

Haario, H., Laine, M., Lehtinen, M., Saksman, E. and Tamminen, J., 2004, MCMC methods for high dimensional inversion in remote sensing, *J. R. Statist. Soc.*, **66**, 591–607.

Harwood, J. M. and Malin, S. R. C., 1977, Sunspot cycle influence on the geomagnetic field, *Geophys. J. R. astr. Soc.*, **50**, 605–619.

Honkura, Y. and Matsushima, M., Electromagnetic response of the mantle to long-period geomagnetic variations over the globe, *Earth Planets Space*, **50**, 651–662.

Gelman, A., Carlin, J. B., Stern, H. S. and Rubin, D. B., 2004. *Bayesian data analysis*, 2nd ed., Chapman & Hall/CRC, Boca Raton, 668 pp.

Grandis, H., Menvielle, M. and Roussignol, M., 1999, Bayesian inversion with Markov chains–I.: The magnetotelluric one-dimensional case, *Geoph. J. Int.*, **138**, 757–768.

Khan, A., Connolly, J. A. D. and Olsen, N., 2006, Constraining the composition and thermal state of the mantle beneath Europe from inversion of long-period electromagnetic sounding data, *J. Geophys. Res.*, **111**, B10102, doi:10.1029/2006JB004270.

Kuvshinov, A. and Olsen, N., 2006, A global model of mantle conductivity derived from 5 years of CHAMP, Ørsted, and SAC-C magnetic data, *Geophys. Res. Lett.*, **33**, L18301.

Larsen, J., 1975, Low frequency (0.1–6. cpd) electromagnetic study of deep mantle electrical conductivity beneath the Hawaiian Islands, *Geophys. J. R. astr. Soc.*, **43**, 17–46.

Medin, A. E., Parker, R. L. and Constable, S., 2007, Making sound inferences from geomagnetic sounding, *Phys. Earth Planet. Int.*, **160**, 51–59.

Olsen, N., 1998, The electrical conductivity of the mantle beneath Europe derived from C-responses from 3 to 720 hr, *Geophys. J. Int.*, **133**, 298–308.

Olsen, N., 1999a, Long-period (30 days–1 year) electromagnetic sounding and the electrical conductivity of the lower mantle beneath Europe, *Geoph. J. Int.*, **138**, 179–187.

Olsen, N., 1999b, Induction studies with satellite data, *Surv. Geophys.*, **20**, 309–340.

Parker, R. L., 1980, The inverse problem of electromagnetic induction: existence and construction of solutions based on incomplete data, *J. Geophys. Res.*, **85**, 4421–4428.

Portniaguine, O. and Zhdanov, M. S., 1999, Focusing geophysical inversion images, *Geophysics*, **64** (3), 874–887.

Praus, O., Červ, V., Kováčiková, S., Pek, J. and Pěčová, J., 2004, Long period geomagnetic variations and electrical conductivity at upper mantle depths, in *Abstracts 17th International Workshop on Electromagnetic Induction in the Earth*, No. 129, Hyderabad India, October 18-23, 2004. Available as Extended Abstract at http://www.emindia2004.org/S5-P11-Praus.pdf.

Roberts, R.G., 1984, The long period electromagnetic response for the Earth, *Geophys. J.R. astr. Soc.*, **78**, 547–572.

Schmucker, U., 1999, A spherical harmonic analysis of solar daily variations in the years 1964–1965: Response estimates and source fields for global induction—II. Results, *Geophys. J. Int.*, **136**, 455–476.

Schultz, A. and J.C. Larsen, 1987, On the electrical conductivity of the mid-mantle: 1. Calculation of equivalent scalar magnetotelluric response functions, *Geophys. J.R. astr. Soc.*, **88**, 733–761.

Semenov, V. Yu., 1998, Regional conductivity structures of the Earth's mantle, *Publ. Inst. Geoph. Pol. Acad. Sci.*, C-95 (302), pp. 1–119.

Semenov, V. Yu. and Jóźwiak, W., 1999, Model of the geoelectrical structure of the mid- and lower mantle in the Europe-Asia region, *Geophys. J. Int.*, **138**, 549–552.

Ulrych, T. J., Sacchi, M. D. and Woodbury, A., 2001, A Bayes tour of inversion: A tutorial, *Geophysics*, **66** (1), 55–69.

Velímský, J., Martinec, Z. and Everett, M., 2006, Electrical conductivity in the Earth's mantle inferred from CHAMP satellite measurements—I. Data processing and 1-D inversion, *Geophys. J. Int.*, **166**, 529–542.

Weidelt, P., 1972, The inverse problem of geomagnetic induction, *Z. Geophys.*, **38**, 257–289.